

Reactions Involving Carbon Dioxide and Mixed
Amido–Phosphido Dinuclear Compounds:
 $M_2(NMe_2)_4(PR_2)_2(M\equiv M)$, Where $M = Mo$ and W .
Comparative Study of the Insertion of Carbon Dioxide into
Metal–Nitrogen and Metal–Phosphorus Bonds

W. E. Buhro,^{†,1} M. H. Chisholm,^{*,†} J. D. Martin,[†] J. C. Huffman,[†] K. Folting,[†] and
W. E. Streib[†]

Contribution from the Department of Chemistry and the Molecular Structure Center, Indiana
University, Bloomington, Indiana 47405. Received January 26, 1989

Abstract: 1,2- $M_2(NMe_2)_4(P(t-Bu)_2)_2$ compounds react with CO_2 (>4 equiv) to yield initially $M_2(O_2CNMe_2)_2(O_2CP(t-Bu)_2)_2(NMe_2)_2$, where $M = Mo$ and W . The reaction occurs rapidly at room temperature in solution and even as a gas/solid heterogeneous reaction. The molybdenum compound is labile to ligand-exchange reactions in solution, and attempts to grow good quality crystals yielded $Mo_2(O_2CP(t-Bu)_2)_4 \cdot 2C_6H_6$, a compound having a Mo–Mo quadruple bond supported by a paddle-wheel arrangement of four phosphinecarboxylate ligands that span the M–M bond. The compound $W_2(O_2CNMe_2)_2(O_2CP(t-Bu)_2)_2(NMe_2)_2$ has been characterized in the solid state and shown to contain a $(W\equiv W)^{6+}$ central unit, 2.29 (1) Å, with a pair of O_2CNMe_2 ligands that span the W–W bond. The phosphinecarboxylates form one short, 2.10 (1) Å, and one long 2.67 (1) Å, W–O bond. The coordination at each tungsten atom involves a distorted square-planar WO_3N moiety with an additional weak O–W bond (2.67 (1) Å) along the W–W axis. A related reaction occurs between 1,2- $W_2(NMe_2)_4(PCy_2)_2$ and CO_2 , initially giving $W_2(O_2CNMe_2)_2(O_2CPCy_2)_2(NMe_2)_2$, where Cy = cyclohexyl, which appears, based on NMR data, to be structurally related to $W_2(O_2CNMe_2)_2(O_2CP(t-Bu)_2)_2(NMe_2)_2$. In solution an isomerization occurs to give one of two isomers that are formulated as having phosphinecarboxylates that bridge the $(W\equiv W)^{6+}$ unit by use of P- and O-to-W bonds. Mechanistic studies employing the use of $^{13}CO_2$ have established that at low temperatures CO_2 preferentially attacks the phosphido ligand (with respect to the amido ligands) giving an initially P-bound phosphinecarboxylate that then rearranges to the O-bound form of the ligand. Comparisons are made with earlier work involving the reactions between metal amides and CO_2 . Crystal data (i) for $Mo_2(O_2CP(t-Bu)_2)_4 \cdot 2C_6H_6$ at $-155^\circ C$: $a = 13.731$ (21) Å, $b = 12.789$ (17) Å, $c = 15.835$ (23) Å, $\beta = 94.86$ (8)°, $Z = 2$, $d_{\text{calcd}} = 1.324$ g cm^{-3} , space group $P2_1/n$. (ii) for $W_2(O_2CNMe_2)_2(O_2CP(t-Bu)_2)_2(NMe_2)_2$ at $-151^\circ C$: $a = 15.455$ (7) Å, $b = 15.786$ (7) Å, $c = 8.502$ (4) Å, $\alpha = 97.22$ (2)°, $\beta = 97.86$ (2)°, $\gamma = 101.22$ (2)°, $Z = 2$, $d_{\text{calcd}} = 1.686$ g cm^{-3} , space group $P\bar{1}$.

For some time we have been investigating the chemistry of metal–metal multiple bonds, specifically those of the M_2L_6 triple-bonded dimers, $M = Mo$ and W .² The influence of the ligands L on the triple bond has been addressed and numerous investigations have probed the activation of small organic molecules at the dinuclear center. This $(M\equiv M)^{6+}$ unit also affords a well-defined template for a comparison of the chemistry of the ancillary metal–ligand bonds. The mixed phosphido–amido compounds, 1,2- $M_2(NMe_2)_4(PR_2)_2$, I, ($M = Mo, W$; $R = t-Bu, Cy$) present the opportunity to compare the metal–nitrogen (amido) and metal–phosphorus (phosphido) bonds. Having previously demonstrated a competitive π -donation, $NMe_2 > PR_2$, by structural and spectroscopic studies,^{3,4} we have attempted to compare NR_2 and PR_2 ligands on the basis of chemical reactivity.

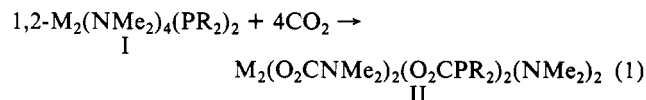
The formal insertion of CO_2 into M– NR_2 bonds yields the corresponding *N,N*-dialkylcarbamate ligands. Earlier work from this laboratory demonstrated that this formal insertion of CO_2 into metal–amido bonds is frequently catalyzed by fortuitous amounts of amine,⁵ though as Lappert and co-workers⁶ noted there is the possibility of a direct insertion via an electrophilic attack at the nitrogen lone pair. Previous investigations have suggested that PR_2 groups might also undergo formal CO_2 insertion to give phosphinecarboxylate (O_2CPR_2) ligands^{7–9} by mechanisms analogous to those invoked for the formal insertion of CO_2 into metal–amido bonds.

In this paper we report the preparation of $M_2(O_2CNMe_2)_2(O_2CPR_2)_2(NMe_2)_2$ (IIa: $M = Mo, R = t-Bu$. IIb: $M = W, R = t-Bu$. IIc: $M = W, R = Cy$) and related compounds from I and the unexpected decomposition of IIa to give $Mo_2(O_2CP(t-Bu)_2)_4$ (III). To our knowledge IIb and III are the first structurally characterized examples of compounds containing

phosphinecarboxylate ligands. A series of labeling studies and ligand-exchange reactions indicate the direct attack by CO_2 on the phosphido ligands and variable-temperature experiments demonstrate a more facile insertion relative to the metal–amido bonds. A preliminary communication reporting the structure of III has appeared.⁷

Results and Discussion

Synthesis. Phosphido–amido complexes I and 4 equiv of CO_2 react both in hydrocarbon solutions and in the solid state at room temperature, to yield the air- and moisture-sensitive complexes with the molecular formula $M_2(O_2CNMe_2)_2(O_2CPR_2)_2(NMe_2)_2$, II, as shown in eq 1.



Variable-temperature ^{13}C NMR spectroscopic studies reveal that the insertion of CO_2 into both metal–phosphido and met-

(1) Present address: Department of Chemistry, Washington University, St. Louis, MO 63130.

(2) Chisholm, M. H. *Angew. Chem., Int. Ed. Engl.* 1986, 25, 21.

(3) Buhro, W. E.; Chisholm, M. H.; Folting, K.; Huffman, J. C. *J. Am. Chem. Soc.* 1987, 109, 905.

(4) Buhro, W. E.; Chisholm, M. H.; Folting, K.; Huffman, J. C.; Martin, J. D.; Streib, W. E., manuscript in preparation.

(5) Chisholm, M. H.; Extine, M. W. *J. Am. Chem. Soc.* 1977, 99, 792, and references therein.

(6) Lappert, M. F.; Prokai, B. *Adv. Organomet. Chem.* 1967, 5, 224.

(7) Buhro, W. E.; Chisholm, M. H.; Huffman, J. C. *Inorg. Chem.* 1987, 26, 3087.

(8) Baker, R. T. *Abstracts of Papers*, 192nd National Meeting of the American Chemical Society, Anaheim, CA; American Chemical Society: Washington, DC, 1987; INOR-96.

(9) Kuchen, W.; Buchwald, H. *Chem. Ber.* 1959, 92, 227.

[†]Department of Chemistry.

^{*}Molecular Structure Center.

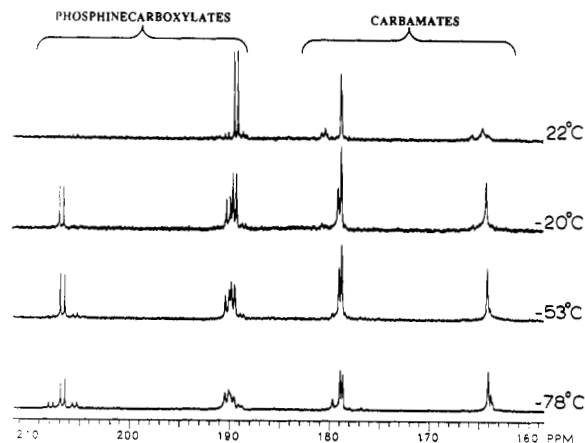
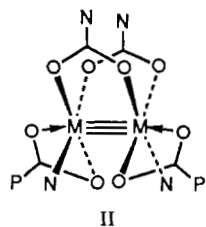


Figure 1. Variable-temperature $^{13}\text{C}\{^1\text{H}\}$ NMR monitoring of the reaction of I ($M = \text{W}$, $R = t\text{-Bu}$) with 4 equiv of $^{13}\text{CO}_2$ as a function of temperature. Bridging carbamate ligands typically appear between 180 and 174 ppm while resonances for dangling ($\eta^1\text{-O}$ -bound) and chelating ($\eta^2\text{-O}$ -bound) carbamate ligands are found between 166 and 160 ppm.

al-amido bonds is rapid even at -78°C . This is apparent from the presence of the carbamate singlets and phosphinecarboxylate doublets as shown in Figure 1. Upon warming, this reaction proceeds to give II as the kinetically accessible thermodynamic product. The carbamate ligands evidently bridge the metal-metal bond. This is deduced from the downfield shift, with respect to chelating and dangling carbamate ligands, in the ^{13}C NMR spectrum for the carbamate O_2C carbon nuclei due to the magnetic anisotropy of the metal-metal triple bond.¹⁰ The lack of $\nu(\text{CO})$ above 1600 cm^{-1} in the infrared spectrum further indicates that both carbamates and phosphinecarboxylates are bound in an η^2 -fashion consistent with the structure diagrammatically shown.

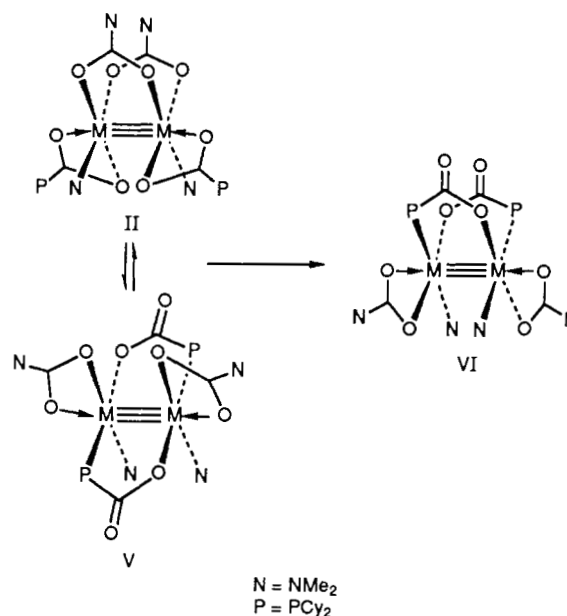


$\text{Mo}_2(\text{O}_2\text{CNMe}_2)_2(\text{O}_2\text{CP}(t\text{-Bu})_2)_2(\text{NMe}_2)_2$ (IIa) is prepared according to eq 1 and may be isolated from hexane in a 60% yield. Our attempts to crystallize IIa have been frustrated by its slow decomposition in solution at ambient temperature to give several new species (by NMR spectroscopy). One decomposition product readily crystallizes in small amounts (0.08–0.10 molar equiv based on IIa) from C_6H_6 and has been identified as $\text{Mo}_2(\text{O}_2\text{CP}(t\text{-Bu})_2)_4 \cdot 2\text{C}_6\text{H}_6$ (III- $2\text{C}_6\text{H}_6$) by spectroscopic analysis and an X-ray crystallographic study. An independent synthesis of III from MoCl_3 , $\text{LiP}(t\text{-Bu})_2$, and CO_2 was also developed (25% yield; see Experimental Section). Initially it was thought that the instability of IIa might result from reversible CO_2 insertion and deinsertion. However, neither II nor III undergoes exchange¹¹ with $^{13}\text{CO}_2$ over the course of several weeks. Nevertheless $^{13}\text{CO}_2$ is incorporated into some of the products during the decomposition of nonlabeled IIa in the presence of $^{13}\text{CO}_2$.

$\text{W}_2(\text{O}_2\text{CNMe}_2)_2(\text{O}_2\text{CP}(t\text{-Bu})_2)_2(\text{NMe}_2)_2$ (IIb) is prepared according to eq 1, in the solid state, or in hydrocarbon solutions, and has been recrystallized from hexane in a 61% yield. Unlike its Mo analogue, IIb is inert with respect to decomposition in hydrocarbon solvents under ambient conditions for several weeks.

When exposed to additional CO_2 , IIb reacts incompletely to give a new product, 30–50% by NMR, which, by spectroscopic characterization, has the molecular formula $\text{W}_2(\mu\text{-}$

Scheme I



$\text{O}_2\text{CNMe}_2)_2(\text{O}_2\text{CNMe}_2)_2(\text{O}_2\text{CP}(t\text{-Bu})_2)_2$ (IV). The conditions required to drive this reaction to completion are as yet unclear, but the reaction of nonlabeled IIb with $^{13}\text{CO}_2$ exhibits ^{13}C incorporation into IV with subsequent scrambling of $^{13}\text{CO}_2$ between carbamates and phosphinecarboxylates. No $^{13}\text{CO}_2$ is incorporated into IIb. This precludes the existence of an equilibrium involving IIb and IV.

$\text{W}_2(\text{O}_2\text{CNMe}_2)_2(\text{O}_2\text{CPCy}_2)_2(\text{NMe}_2)_2$ (IIc) is synthesized according to eq 1 but is unstable with respect to isomerization in solution. Two products, V and VI, may be isolated from the isomerization of IIc depending on the reaction conditions. Even at -20°C , in a toluene solution, IIc is in equilibrium with a second isomer V. Because of its lower solubility, V may be isolated as an impure powder (>90% V) from toluene or hexane solutions of an equilibrium mixture of IIc and V. When the toluene solution of IIc and V is warmed to room temperature, both IIc and V isomerize to a third product, VI, which precipitates as a pure microcrystalline material.

The ^{13}C NMR spectra of both V and VI suggest that the carbamate ligands have migrated from bridging to chelating or dangling positions (see Experimental Section). The presence of tungsten satellites in the $^{31}\text{P}\{^1\text{H}\}$ NMR spectra due to coupling to ^{183}W , $I = 1/2$, 14% natural abundance, $J_{31\text{P},183\text{W}} = 235$ and 247 Hz, respectively, and the appearance of $\nu(\text{CO})$ at 1670 in the infrared spectrum of both V and VI suggest that the phosphinecarboxylates are bound through P and likely occupy bridging positions. Precedence for the formation of M–P bonds at the expense of M–O bonds is found in the work of Andersen¹² and Cotton.¹³ Tertiary phosphines were seen to force carboxylate ligands, spanning a Mo–Mo quadruple bond, into dangling modes of coordination: $\text{Mo}_2(\text{O}_2\text{CCF}_3)_4 + \text{PR}_3 \rightarrow \text{Mo}_2(\mu\text{-O}_2\text{CCF}_3)_2(\text{O}_2\text{CCF}_3)_2(\text{PR}_3)_2$.

Previous work has demonstrated a facile exchange between carbamates occupying bridging and chelating or dangling configurations at $(\text{W}=\text{W})^{6+}$ centers.¹⁴ Thus, we suggest that the equilibrium between IIc and V is a result of the reversible interchange of bridging and dangling carbamates and phosphinecarboxylates. The more stable isomer VI, formed at or above room temperature, is likely a result of a rotation about the metal-metal bond, which must be coupled with the above. This series of isomerizations is shown diagrammatically in Scheme I. Note

(10) Chisholm, M. H.; Cotton, F. A. *Acc. Chem. Res.* **1978**, *11*, 356.

(11) Exchange is used to define the scrambling of CO_2 moieties in and out of O_2CNMe_2 ligands noted in earlier studies. See ref 5.

(12) Girolami, G. S.; Mainz, V. V.; Andersen, R. A. *Inorg. Chem.* **1980**, *19*, 805.

(13) Cotton, F. A.; Lay, D. G. *Inorg. Chem.* **1981**, *20*, 935.

(14) Chisholm, M. H.; Cotton, F. A.; Extine, M. W.; Stults, R. G. *Inorg. Chem.* **1977**, *16*, 603.

Table I. Atomic Positional Parameters for W₂(O₂CNMe₂)₂(O₂CP(*t*-Bu))₂(NMe₂)₂

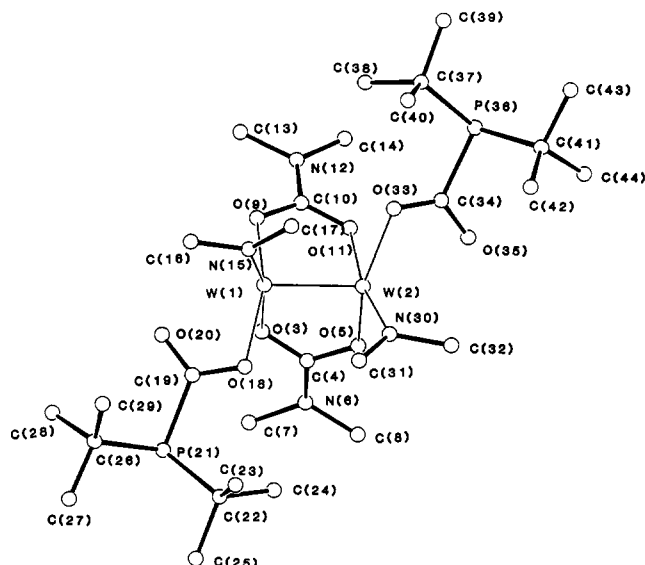
atom	10 ⁴ x	10 ⁴ y	10 ⁴ z	10B ₁₀₀
W(1)	3721 (1)	2238 (1)	7024 (1)	20
W(2)	4790 (1)	2246.7 (5)	9180 (1)	19
O(3)	3268 (10)	851 (9)	7158 (18)	35
C(4)	3450 (13)	619 (13)	8528 (22)	22
O(5)	4155 (10)	1050 (9)	9572 (19)	36
N(6)	3013 (11)	-116 (10)	8883 (18)	25
C(7)	2202 (17)	-612 (16)	7801 (29)	42
C(8)	3249 (18)	-384 (14)	10455 (25)	44
O(9)	4441 (9)	1711 (8)	5448 (15)	24
C(10)	5118 (13)	1418 (11)	5995 (23)	22
O(11)	5369 (8)	1459 (8)	7517 (15)	19
N(12)	5582 (10)	1062 (9)	4978 (19)	19
C(13)	5287 (15)	965 (12)	3238 (21)	24
C(14)	6377 (15)	806 (13)	5530 (25)	29
N(15)	3871 (12)	3440 (10)	6611 (21)	35
C(16)	3297 (15)	3648 (14)	5316 (28)	32
C(17)	4547 (15)	4220 (12)	7472 (22)	28
O(18)	2579 (9)	2272 (10)	8049 (18)	35
C(19)	1929 (18)	1909 (19)	6890 (32)	50
O(20)	2060 (11)	1784 (12)	5487 (19)	44
P(21)	795 (5)	1416 (5)	7353 (10)	49
C(22)	855 (17)	1834 (21)	9573 (35)	55
C(23)	1099 (22)	2814 (23)	10159 (41)	74
C(24)	1562 (20)	1401 (24)	10432 (41)	71
C(25)	-88 (22)	1435 (25)	9951 (45)	77
C(26)	102 (19)	1984 (19)	5988 (41)	62
C(27)	-831 (17)	1918 (20)	6432 (35)	57
C(28)	-1 (25)	1462 (29)	4346 (48)	99
C(29)	544 (23)	2955 (24)	5948 (42)	75
N(30)	4492 (10)	2989 (9)	10919 (18)	18
C(31)	3822 (15)	3508 (14)	10965 (25)	31
C(32)	5039 (17)	3103 (14)	12497 (28)	36
O(33)	5956 (8)	3115 (9)	8868 (16)	23
C(34)	6587 (13)	2907 (13)	9647 (26)	26
O(35)	6495 (9)	2384 (8)	10634 (16)	27
P(36)	7751 (4)	3290 (4)	9257 (7)	25
C(37)	7622 (14)	4041 (13)	7668 (24)	27
C(38)	7048 (16)	3400 (17)	6186 (29)	45
C(39)	8541 (14)	4336 (15)	7228 (27)	34
C(40)	7217 (15)	4796 (14)	8040 (30)	36
C(41)	8203 (15)	3976 (14)	11318 (27)	32
C(42)	7601 (15)	4483 (13)	12035 (25)	29
C(43)	9123 (16)	4591 (17)	11236 (28)	43
C(44)	8421 (18)	3314 (16)	12421 (25)	43

Table II. Selected Bond Distances (Å) for W₂(O₂CNMe₂)₂(O₂CP(*t*-Bu))₂(NMe₂)₂

A	B	distance	A	B	distance
W(1)	W(2)	2.2904 (15)	P(36)	C(34)	1.871 (21)
W(1)	O(3)	2.188 (14)	P(36)	C(37)	1.922 (20)
W(1)	O(9)	2.053 (14)	P(36)	C(41)	1.904 (23)
W(1)	O(18)	2.080 (14)	O(3)	C(4)	1.276 (23)
W(1)	O(20)	2.635 (17)	O(5)	C(4)	1.317 (23)
W(1)	N(15)	1.948 (16)	O(9)	C(10)	1.278 (23)
W(2)	O(5)	2.042 (13)	O(11)	C(10)	1.289 (23)
W(2)	O(11)	2.164 (12)	O(18)	C(19)	1.29 (3)
W(2)	O(33)	2.112 (12)	O(20)	C(19)	1.24 (3)
W(2)	N(30)	1.932 (15)	O(33)	C(34)	1.225 (22)
P(21)	C(19)	1.89 (3)	O(35)	C(34)	1.252 (23)
P(21)	C(22)	1.90 (3)	N(6)	C(4)	1.316 (24)
P(21)	C(26)	1.90 (3)	N(12)	C(10)	1.335 (25)

all the isomers shown in Scheme I share a common template in which four metal-ligand bonds lie in the *xy* plane. In this way metal *s*, *p_x*, *p_y* and *d_{x²-y²}* orbitals may be used in M-L σ-bonding and the metal *d_{xy}* orbital is available for π-bonding with the nitrogen *p_x* orbital. The additional weak axial interaction with an oxygen atom of a phosphine carboxylate or carbamate uses the metal *p_z* atomic orbitals. This bonding pattern finds a parallel in that noted previously for W₂Me₂(O₂CNEt₂)₄, W₂(O₂CNMe₂)₆ and W₂(O₂C-*t*-Bu)₆.

Molecular and Solid-State Structures. (a) W₂(O₂CNMe₂)₂(O₂CP(*t*-Bu))₂(NMe₂)₂ (IIB). An X-ray crystallographic study

**Figure 2.** Ball-and-stick drawing of the W₂(O₂CNMe₂)₂(O₂CP(*t*-Bu))₂(NMe₂)₂ molecule giving the atom number scheme.**Table III.** Selected Bond Angles (Degrees) for the W₂(O₂CNMe₂)₂(O₂CP(*t*-Bu))₂(NMe₂)₂ Molecule

A	B	C	angle
W(2)	W(1)	O(3)	85.6 (4)
W(2)	W(1)	O(9)	91.8 (4)
W(2)	W(1)	O(18)	103.3 (4)
W(2)	W(1)	O(20)	151.5 (4)
W(2)	W(1)	N(15)	106.5 (5)
O(3)	W(1)	O(9)	80.4 (5)
O(3)	W(1)	O(18)	79.6 (6)
O(3)	W(1)	O(20)	74.0 (6)
O(3)	W(1)	N(15)	167.4 (7)
O(9)	W(1)	O(18)	153.8 (6)
O(9)	W(1)	O(20)	103.9 (5)
O(9)	W(1)	N(15)	102.2 (7)
O(18)	W(1)	O(20)	54.1 (6)
O(18)	W(1)	N(15)	94.0 (7)
O(20)	W(1)	N(15)	93.5 (6)
W(1)	W(2)	O(5)	92.2 (5)
W(1)	W(2)	O(11)	86.0 (3)
W(1)	W(2)	O(33)	106.3 (4)
W(1)	W(2)	N(30)	104.4 (5)
O(5)	W(2)	O(11)	82.5 (6)
O(5)	W(2)	O(33)	150.7 (6)
O(5)	W(2)	N(30)	100.1 (6)
O(11)	W(2)	O(33)	76.5 (5)
O(11)	W(2)	N(30)	169.2 (6)
O(33)	W(2)	N(30)	97.1 (5)
C(19)	P(21)	C(22)	104.6 (12)
C(19)	P(21)	C(26)	97.9 (13)
C(22)	P(21)	C(26)	112.9 (15)
C(34)	P(36)	C(37)	104.3 (9)
C(34)	P(36)	C(41)	96.1 (10)
C(37)	P(36)	C(41)	109.9 (9)
W(1)	O(3)	C(4)	116.4 (13)
W(2)	O(5)	C(4)	118.4 (13)
W(1)	O(9)	C(10)	119.4 (13)
W(2)	O(11)	C(10)	118.9 (12)
W(1)	O(18)	C(19)	104.0 (15)
W(1)	O(20)	C(19)	79.6 (16)
W(2)	O(33)	C(34)	106.5 (12)
W(1)	N(15)	C(16)	119.8 (14)
W(1)	N(15)	C(17)	128.1 (13)
W(2)	N(30)	C(31)	131.9 (13)
W(2)	N(30)	C(32)	117.7 (13)
C(31)	N(30)	C(32)	110.4 (16)

of IIB reveals a complex with approximate C₂ symmetry. A ball-and-stick view of the molecular structure is shown in Figure 2, and a view of the molecule down the W-W bond is shown in Figure 3. The refined positional and thermal parameters for all

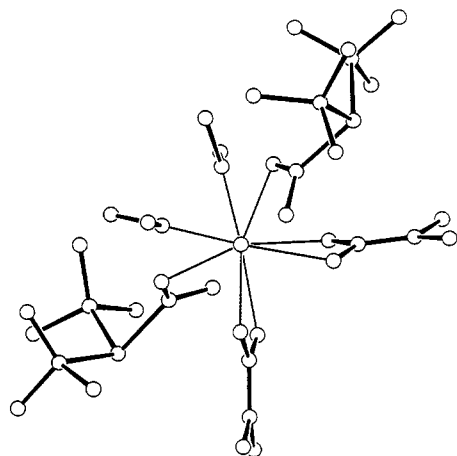


Figure 3. View of the $W_2(O_2CNMe_2)_2(O_2CP(t-Bu)_2)_2(NMe_2)_2$ molecule down the W-W bond emphasizing the skewed geometry of the two WO_3N units and the pyramidal geometry at phosphorus.

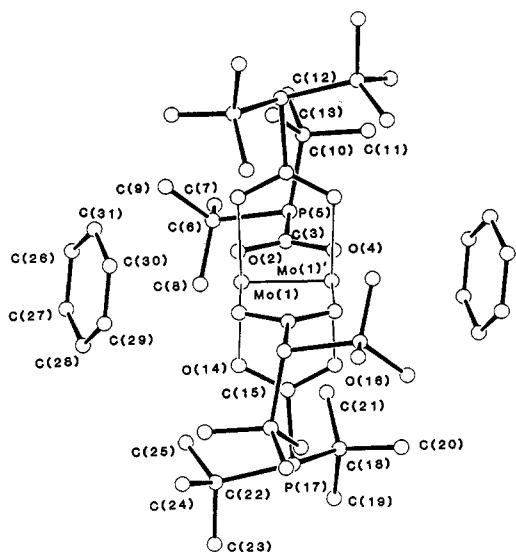


Figure 4. Ball-and-stick drawing of $Mo_2[O_2CP(t-Bu)_2]_4 \cdot 2C_6H_6$ giving the atom number scheme. Selected distances (Å): Mo-Mo = 2.092 (3), Mo-O (av) = 2.107 (9), O-C (av) = 1.27 (1), and O₂C-P (av) = 1.860 (5). Selected angles (deg): Mo-Mo-O (av) = 91.81 (8), O-Mo-O (av) = 89.95 (15), O-C-O (av) = 121.5 (4).

atoms are reported in Table I, the bond distances are reported in Table II, and the bond angles are reported in Table III. The W-W distance of 2.290 (1) Å is consistent with other d^3-d^3 ($W \equiv W$)⁶⁺ units. The carbamate ligands asymmetrically span the metal-metal bond ($W-O = 2.05$ Å, $W-O' = 2.18$ Å), with each long W-O bond being trans to a terminal amido ligand. Similar trans influences of amido ligands have been reported elsewhere.¹⁵ The carbamate C-N bond length of 1.33 (2) Å is indicative of a carbon-nitrogen double bond.¹⁶ By contrast, the C-P bond length of the phosphinecarboxylate, 1.88 (3) Å, is approximately equal that of the sum of their covalent radii.¹⁷ Of further note is the planarity of the O₂CNC₂ unit in the carbamate ligand as opposed to the distinct pyramidal geometry of the phosphorous atom of the phosphinecarboxylate. The summation of bond angles about P are 310 and 315°. This implies a greater delocalization of the N lone pair within the π -system of the Me₂NCO₂ ligands relative to the P lone pair in the $(t-Bu)_2PCO_2$ ligands.

(15) Ahmed, K. J.; Chisholm, M. H.; Foltling, K.; Huffman, J. C. *Inorg. Chem.* **1985**, *24*, 4039.

(16) For C-N distances in related compounds, see: Chisholm, M. H.; Extine, M. W. *J. Am. Chem. Soc.* **1977**, *99*, 782.

(17) This can be ascertained from the P-C bond distances in this molecule assuming a C_{sp²} radius of 0.70 Å and C_{sp³} of 0.77 Å: Kitchutsu, K. *MTP Int. Rev. Sci., Phys. Chem., Ser. One* **1972**, *11*, 221.

Table IV. Fractional Coordinates and Isotropic Thermal Parameters for $Mo_2(O_2CP(t-Bu)_2)_4 \cdot 2C_6H_6$

atom	10 ⁴ x	10 ⁴ y	10 ⁴ z	10B _{iso}
Mo(1)	4912.2 (2)	4201.8 (3)	4871.5 (2)	12
O(2)	4151 (2)	3977 (2)	5952 (2)	14
C(3)	4024 (3)	4760 (3)	6416 (2)	14
O(4)	4330 (2)	5670 (2)	6233 (2)	15
P(5)	3405 (1)	4669 (1)	7416 (1)	17
C(6)	2812 (3)	3336 (3)	7343 (3)	20
C(7)	2155 (3)	3269 (4)	8080 (3)	27
C(8)	2147 (3)	3353 (4)	6520 (3)	29
C(9)	3479 (3)	2389 (3)	7353 (3)	21
C(10)	4564 (3)	4642 (3)	8156 (3)	21
C(11)	4854 (4)	5790 (4)	8298 (3)	35
C(12)	4339 (4)	4185 (4)	9014 (3)	26
C(13)	5430 (3)	4063 (4)	7832 (3)	25
O(14)	3573 (2)	4451 (2)	4155 (2)	14
C(15)	3264 (3)	5394 (3)	4083 (2)	15
O(16)	3764 (2)	6156 (2)	4409 (2)	15
P(17)	2103 (1)	5748 (1)	3465 (1)	14
C(18)	1515 (3)	6481 (3)	4338 (3)	17
C(19)	418 (3)	6545 (4)	4104 (3)	22
C(20)	1940 (3)	7588 (3)	4320 (3)	19
C(21)	1706 (3)	6025 (4)	5230 (3)	22
C(22)	1501 (3)	4442 (3)	3222 (3)	19
C(23)	515 (3)	4642 (4)	2698 (3)	25
C(24)	2158 (3)	3895 (4)	2622 (3)	23
C(25)	1336 (3)	3739 (3)	3980 (3)	22
C(26)	9026 (5)	3952 (4)	392 (4)	43
C(27)	8285 (4)	3838 (4)	-241 (4)	43
C(28)	8465 (4)	3378 (4)	-995 (4)	38
C(29)	9393 (4)	3053 (4)	-1112 (3)	33
C(30)	10129 (4)	3171 (4)	-484 (3)	30
C(31)	9955 (4)	3606 (4)	274 (3)	36

Table V. Selected Bond Distances (Å) for $Mo_2(O_2CP(t-Bu)_2)_4 \cdot 2C_6H_6$

A	B	distance	A	B	distance
Mo(1)	Mo(1)	2.092 (3)	P(17)	C(15)	1.855 (5)
Mo(1)	O(2)	2.099 (4)	P(17)	C(18)	1.905 (4)
Mo(1)	O(4)	2.116 (4)	P(17)	C(22)	1.888 (5)
Mo(1)	O(14)	2.101 (4)	O(2)	C(3)	1.264 (5)
Mo(1)	O(16)	2.112 (4)	O(4)	C(3)	1.279 (5)
P(5)	C(3)	1.864 (5)	O(14)	C(15)	1.280 (5)
P(5)	C(6)	1.889 (5)	O(16)	C(15)	1.276 (5)
P(5)	C(10)	1.896 (5)			

Table VI. Selected Bond Angles (Degrees) for $Mo_2(O_2CP(t-Bu)_2)_4 \cdot 2C_6H_6$

A	B	C	angle
Mo(1)	Mo(1)	O(2)	91.86 (8)
Mo(1)	Mo(1)	O(4)	91.64 (8)
Mo(1)	Mo(1)	O(14)	92.19 (8)
Mo(1)	Mo(1)	O(16)	91.53 (8)
O(2)	Mo(1)	O(4)	176.50 (10)
O(2)	Mo(1)	O(14)	89.28 (15)
O(2)	Mo(1)	O(16)	89.77 (15)
O(4)	Mo(1)	O(14)	90.66 (15)
O(4)	Mo(1)	O(16)	90.07 (15)
O(14)	Mo(1)	O(16)	176.19 (10)
C(3)	P(5)	C(6)	103.26 (18)
C(3)	P(5)	C(10)	96.10 (21)
C(6)	P(5)	C(10)	110.87 (19)
C(15)	P(17)	C(18)	97.78 (20)
C(15)	P(17)	C(22)	103.50 (20)
C(18)	P(17)	C(22)	112.16 (19)
Mo(1)	O(2)	C(3)	117.90 (24)
Mo(1)	O(4)	C(3)	116.87 (24)
Mo(1)	O(14)	C(15)	117.35 (24)
Mo(1)	O(16)	C(15)	117.52 (25)
P(5)	C(3)	O(2)	122.7 (3)
P(5)	C(3)	O(4)	115.60 (28)
O(2)	C(3)	O(4)	121.7 (3)

(b) $Mo_2(O_2CP(t-Bu)_2)_4$ (III). The molecular structure of III (Figure 4) has previously been reported.⁷ Atomic positional

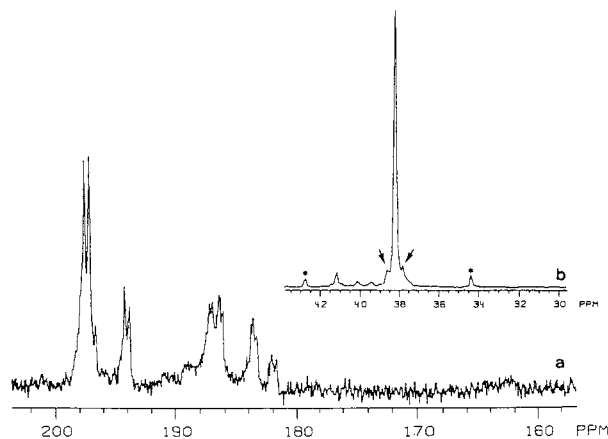


Figure 5. (a) $^{13}\text{C}\{^1\text{H}\}$ NMR spectrum of the reaction of I ($M = \text{W}$, $R = t\text{-Bu}$) with 1 equiv of $^{13}\text{CO}_2$ at -120°C in a toluene- d_8 /Freon-12 solution. (b) $^{31}\text{P}\{^1\text{H}\}$ NMR spectrum of the reaction of I ($M = \text{W}$, $R = t\text{-Bu}$) with 1 equiv of $^{12}\text{CO}_2$ at -120°C in a solution of toluene- d_8 /Freon-12. Arrows denote tungsten satellites and resonances marked with * do not exhibit $^{31}\text{P}\text{-}^{13}\text{C}$ coupling when $^{13}\text{CO}_2$ is employed.

parameters are given in Table IV, and selected bond distances and angles are listed in Tables V and VI, respectively. The compound adopts the familiar paddle-wheel geometry of $\text{Mo}_2(\text{O}_2\text{CX})_4(\text{M}^4\text{-M})$ species¹⁸ with unexceptional M-M and M-O distances. The benzene solvate molecules in axial positions are at distances precluding strong bonding interactions (the shortest M-C distance is 3.11 Å).¹⁹ Configurations at P are pyramidal, as shown by the summation of bond angles about P, 310.2–313.4°. The P-CO₂ distances of 1.86 (1) Å are normal P-C single bond lengths.¹⁷

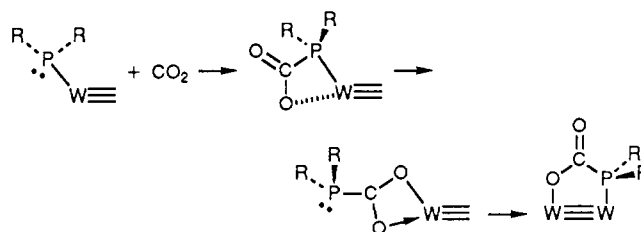
Structural features of both IIb and III demonstrate a lesser degree of delocalization of the P lone pair into the π -system of CO₂ in phosphinecarboxylate ligands than is observed for the N lone pair in carbamate ligands.

Mechanistic Observations. Low-Temperature Experiments. Since the formal insertion of CO₂ into metal-phosphido and metal-amido bonds is rapid even at -78°C , a competition experiment was carried out to interrogate the relative reactivities of these first- and second-row congeners. By monitoring (^{13}C NMR spectroscopy) the reaction of I ($M = \text{W}$, $R = t\text{-Bu}$) with 1 equiv of $^{13}\text{CO}_2$ at -120°C , in a toluene- d_8 /Freon-12 solution, we observed no signals in the carbamate region (180–150 ppm). Only phosphinecarboxylate doublets were observed, which indicates a preferential insertion of $^{13}\text{CO}_2$ into the W-PR₂ bonds. See Figure 5a. Phosphinecarboxylate doublets at $\delta = 194$ and 183 ppm, presumably products of a ligand rearrangement, grow in with time and increased temperature such that at -80°C the resonance at 194 ppm is the major ^{13}C signal.

By following the analogous reaction with $^{12}\text{CO}_2$ (^{31}P NMR; Figure 5b) one observes the major resonance, $\delta = 38.1$ ppm, to be flanked by 14% satellites due to ^{183}W , $I = 1/2$, 14.5% natural abundance ($^1J_{^{31}\text{P}\text{-}^{183}\text{W}} = 116$ Hz) suggesting the initial formation of a P-bound phosphinecarboxylate. This intermediate is thermally unstable and presumably rearranges to an O-bound phosphinecarboxylate due to the thermodynamic preference for W-O bonds. The subsequent rearrangement of IIc to yield the apparent O-, P-bound phosphinecarboxylate leads us to postulate the reaction pathway shown in Scheme II for CO₂ insertion into metal-phosphido bonds at the ($\text{M}\equiv\text{M}$)⁶⁺ center.

CO₂- and Ligand-Exchange Reactions. The above provides strong evidence for the direct insertion of CO₂ into the metal-phosphido bonds. However, fortuitous amounts of phosphine and amine are always present due to trace hydrolysis. Thus, the

Scheme II



possibility of a competing amine/phosphine-catalyzed or -assisted reaction pathway also exists.⁵ Consequently, several CO₂ insertion reactions were examined in the presence of an alternate phosphine, R₂PH.

The ^{31}P chemical shifts of the [($t\text{-Bu}$)₂PCO₂] ligand in IIb, and the [Cy₂PCO₂] ligand in IIc, are separated by ~ 35 ppm (see Experimental Section), similar to the separation in chemical shifts of di-*tert*-butylphosphine, $\delta = 19.9$ ppm, and dicyclohexylphosphine, $\delta = -27.6$ ppm. However, when 4 equiv of CO₂ is added to I ($M = \text{W}$, $R = t\text{-Bu}$) in the presence of an excess of HPCy₂ only a product with ($t\text{-Bu}$)₂PCO₂ ligands is observed, $\delta = 44.4$ ppm, which is IIb.

When exposed to an excess of $^{13}\text{CO}_2$, IIb reacts incompletely (30–50% by NMR) to yield IV. By monitoring this reaction at low temperatures using ^{13}C NMR spectroscopy, we observe that $^{13}\text{CO}_2$ inserts primarily into the metal-amido bonds of IIb at -80°C to yield a dangling or chelating carbamate ($\delta = 164.9$ ppm). At -40°C $^{13}\text{CO}_2$ has been scrambled between the bridging ($\delta = 180.5$ ppm) and chelating or dangling carbamates. Complete exchange with free $^{13}\text{CO}_2$ is never observed, as seen by the apparent "triplets" for the carbamate methyl protons of IV by ^1H NMR. Within an hour at room temperature $^{13}\text{CO}_2$ incorporation into the phosphinecarboxylates is observed ($\delta = 190.3$ ppm, $^1J_{^{31}\text{P}\text{-}^{13}\text{C}} = 28$ Hz). When IIb is allowed to react with an excess of $^{13}\text{CO}_2$ in the presence of free HPCy₂, there is no evidence for any PCy₂ for P($t\text{-Bu}$)₂ exchange.

The incorporation of $^{13}\text{CO}_2$ into some of the decomposition products of IIa offers one further case in which to test for a phosphine-assisted, CO₂-insertion/exchange mechanism. When IIa is allowed to decompose in the presence of an excess of $^{13}\text{CO}_2$ and HPCy₂, one observes by $^{31}\text{P}\{^1\text{H}\}$ NMR not only the profusion of decomposition products with chemical shifts between 44 and 59 ppm corresponding to di-*tert*-butylphosphinecarboxylates but also doublets at 18.9 and 7.7 ppm ($^1J_{^{31}\text{P}\text{-}^{13}\text{C}} = 24$ Hz), which presumably are dicyclohexylphosphinecarboxylates. Not knowing the nature of the products of decomposition, we do not offer any speculation concerning the reaction pathway leading to the formation of Cy₂PCO₂ ligands in these reactions.

Conclusions

The insertion of CO₂ into metal-phosphido bonds to form phosphinecarboxylate ligands, like the formation of carbamate ligands, has been shown to be facile at the ($\text{M}\equiv\text{M}$)⁶⁺ center. Low-temperature studies indicate a kinetic preference for the insertion of CO₂ into metal-phosphido bonds as opposed to metal-amido bonds. Both ligand-exchange reactions and low-temperature studies suggest a direct insertion of CO₂ into metal-phosphido bonds. However, a phosphine-assisted, CO₂-exchange mechanism may, in part, be responsible for the decomposition products of IIa.

Experimental Section

General Procedures, Reagents, and Instrumentation. Our general experimental techniques have been described in detail elsewhere.⁵ All manipulations were carried out under an atmosphere of dry and oxygen-free nitrogen; all solvents were dried and distilled from sodium benzophenone ketyl and stored over molecular sieves. M₂(NMe₂)₄(PR₂)₂ ($M = \text{Mo}$ or W , $R = t\text{-Bu}$ or Cy) was prepared as described elsewhere.^{3,4} ^{13}C -labeled compounds were prepared with 99 atom % $^{13}\text{CO}_2$ obtained from MSD isotopes, which was used without further purification, otherwise bone-dry natural-abundance CO₂ was used. ^1H and ^{13}C NMR spectra were recorded on Nicolet 360 and Varian XL300 instruments. ^{31}P NMR spectra were recorded on a Nicolet 360 instrument. Infrared

(18) Cotton, F. A.; Walton, R. A. In *Multiple Bonds Between Metal Atoms*; Wiley: New York, 1982.

(19) A similar benzene-Cr interaction has been seen in Cr₂(O₂CPh₃)₄·C₆H₆; Cotton, F. A.; Feng, X.; Kibala, P. A.; Matusz, M. *J. Am. Chem. Soc.* **1988**, *110*, 2807.

spectra were recorded on a Perkin-Elmer 283 spectrometer.

Mo₂(O₂CNMe₂)₂(O₂CP(*t*-Bu)₂)₂(NMe₂)₂ (IIa). CO₂ (4.26 mmol) was condensed onto a frozen mixture of 1,2-Mo₂(NMe₂)₄[P(*t*-Bu)₂]₂ (0.200 g, 0.304 mmol) and hexane (6 mL) in a Schlenk flask. The flask was transferred to a room-temperature water bath; the red color faded rapidly and in <2 min a yellow precipitate formed. The mixture was stirred at room temperature for 30 min and then was cooled to 0 °C (30 min) to complete the precipitation. Complex IIa was collected by filtration as a yellow powder, mp 169–176 °C dec (0.151 g, 0.181 mmol, 60%). Anal. Calcd for C₂₈H₆₀Mo₂N₄O₈P₂ (834.64): C, 40.29; H, 7.25. Found: C, 40.18; H, 7.11. IR (KBr, cm⁻¹): 2980 (w), 2940 (m), 2910 (m), 2885 (m), 2860 (m), 2810 (w), 2770 (w), 1575 (s br), 1480 (m), 1544 (m), 1465 (s), 1390 (m), 1366 (w), 1264 (s), 1177 (w), 956 (w), 835 (w), 815 (w), 786 (w), 781 (w), 693 (w), 672 (w), 650 (w), 580 (w), 534 (w), 456 (w), 424 (w). ¹H NMR (room temperature, benzene-*d*₆): δ (N(CH₃)₂) 4.85 (s) and 3.10 (s); (O₂CN(CH₃)₂) 2.83 (s) and 2.63 (s); (P(*t*-Bu)₂) 1.48 (d, ³J_{31P-1H} = 11.1 Hz) and 1.46 ppm (d, ³J_{31P-1H} = 11.2 Hz). ¹³C{¹H} NMR (room temperature, benzene-*d*₆): δ (O₂CP(*t*-Bu)₂) 189.0 (d, ¹J_{13C-31P} = 24.7 Hz); (O₂CNMe₂) 174.8 (s); (N(CH₃)₂) 59.7 (s) and 47.8 (s); (O₂CN(CH₃)₂) 37.2 and 36.8 (s); (PCMe₃)₂ 33.1 (d, ¹J_{13C-31P} = 21.4 Hz) and 32.6 (d, ¹J_{13C-31P} = 23.1 Hz); (P(C(CH₃)₃)₂) 30.8 (d, ²J_{13C-31P} = 12.2 Hz) and 30.7 ppm (d, ²J_{13C-31P} = 12.1 Hz). ³¹P{¹H} NMR (room temperature, benzene-*d*₆): δ 43.0 ppm (s).

Mo₂(O₂CP(*t*-Bu)₂)₂ (III). A. Complex IIa was generated in situ from 1,2-Mo₂(NMe₂)₄[P(*t*-Bu)₂]₂ (0.217, 0.330 mmol) and CO₂ (1 atm) in C₆H₆ (4 mL) at room temperature. A green-yellow solution was rapidly formed and allowed to stand 4 h at room temperature. A small amount of black precipitate was removed by filtration; the filtrate was evaporated to <1 mL and stored at ca. -25 °C for 5 days. Yellow crystals of III·2C₆H₆ were collected from the mother liquor and rinsed with a small amount of C₆H₆, dec pt 213–245 °C (0.032 g, 0.029 mmol). The well-formed crystals of III·2C₆H₆ fracture violently under vacuum, with loss of the solvate. Consequently, the poor CH analysis (below) was likely due to partial solvate loss.

B. A Schlenk flask was charged with MoCl₃ (0.200 g, 0.989 mmol) and cooled to -78 °C, and THF (3 mL) was added. A solution of LiP(*t*-Bu)₂ (0.451 g, 2.97 mmol) in THF (7 mL) was then added dropwise by syringe to the stirring slurry in 10 min. After 45 min at -18 °C, the yellow-brown mixture was transferred to a CO₂/CH₂CN bath (-43 °C) for 40 min to complete the in situ generation of Mo₂[P(*t*-Bu)₂]₂μ-P(*t*-Bu)₂;²⁰ in situ data: ³¹P{¹H} NMR (THF, -35 °C) δ 279.7 (t, ²J_{pp} = 64.8 Hz), 231.7 ppm (t, ²J_{pp} = 64.8 Hz). Reduction of Mo(III) to Mo(II) was accompanied by formation of (*t*-Bu)₂P-P(*t*-Bu)₂.

CO₂ (1 atm) was then added, and the cold bath was removed. The solution was allowed to warm for 30 min and then solvent was evaporated to give a brown gummy residue. The residue was extracted with 15 + 10 mL of hexane; the extracts were filtered and evaporated to a yellow oil. The oil was taken up in C₆H₆ (<1 mL); crystals of III·2C₆H₆ formed upon cooling (ca. -25 °C) overnight (0.136 g, 0.123 mmol, 25%). Anal. Calcd for C₃₆H₇₂Mo₂O₈P₂·2C₆H₆ (1104.96): C, 52.18; H, 7.66. Found: C, 49.90; H, 7.36. IR (KBr, cm⁻¹): 2990 (w), 2941 (m), 2895 (m), 2860 (m), 1469 (m), 1438 (m), 1395 (w), 1388 (m), 1365 (m), 1356 (w), 1309 (s), 1175 (m), 828 (w), 810 (w), 688 (m), 601 (w), 572 (w), 525 (w), 425 (w). ¹H NMR (room temperature, benzene-*d*₆): δ (C₆H₆ solvate) 7.15 (s); (P(*t*-Bu)₂) 1.47 ppm (d, ³J_{31P-1H} = 11.6 Hz). ¹³C{¹H} NMR (room temperature, benzene-*d*₆): δ (O₂CP(*t*-Bu)₂) 192.5 (d, ¹J_{13C-31P} = 31.3 Hz); (C₆H₆ solvate) 128.5; (PCMe₃)₂ 33.9 (d, ¹J_{13C-31P} = 22.8 Hz); (P(C(CH₃)₃)₂) 30.6 ppm (d, ²J_{13C-31P} = 13.3 Hz). ³¹P{¹H} NMR (room temperature, benzene-*d*₆): δ 51.0 ppm (s).

W₂(O₂CNMe₂)₂(O₂CP(*t*-Bu)₂)₂(NMe₂)₂ (IIb). W₂(NMe₂)₄(P(*t*-Bu)₂)₂ (250 mg, 0.300 mmol) was taken up in hexane (10 mL), and 4 equiv (1.200 mmol) of CO₂ was condensed onto the frozen reaction mixture. The reaction mixture was thawed in a dry ice/acetone bath (-78 °C) for 15 min and then gradually allowed to warm to room temperature for 45 min. The volume of solvent was reduced under vacuum until yellow needles began to form. Cooling the solution to -20 °C overnight afforded single crystals. The total crystalline yield was 178 mg (61%).

Alternatively, W₂(NMe₂)₄(P(*t*-Bu)₂)₂ (435 mg, 0.522 mmol) was ground to a powder and placed into a Schlenk flask. CO₂ (4 equiv, 2.09 mmol) was added by vacuum-line techniques. Upon warming to room temperature the yellow powder turned red. After 3 h at room temperature the product, by ¹H NMR spectroscopy, was 100% IIb. Recrystallization from hexane at -20 °C afforded a total crystalline yield of 202 mg (39%). Anal. Calcd for W₂C₂₈H₆₀N₄O₈P₂ (1010.6): C, 33.28; H, 6.00. Found: C, 33.14; H, 6.23. IR (KBr, cm⁻¹): 2992 (m), 2954 (s), 2902 (s), 2874 (s), 2830 (m), 2786 (m), 1581 (s), 1479 (7), 1419 (s),

1395 (m), 1371 (w), 1258 (s), 1182 (w), 966 (m), 839 (w), 818 (w), 792 (w), 684 (w), 655 (m). ¹H NMR (room temperature, toluene-*d*₈): δ (P(*t*-Bu)₂) 1.428 (d, ³J_{31P-1H} = 11.2 Hz) and 1.432 (d, ³J_{31P-1H} = 11.2 Hz); (O₂CN(CH₃)₂) 2.54 (d, ³J_{13C-1H} = 3 Hz) and 2.77 (d, ³J_{13C-1H} = 3 Hz); (N(CH₃)₂) 3.09 (s) and 4.90 ppm (s). ¹³C{¹H} NMR (room temperature, toluene-*d*₈): δ (O₂CNMe₂) 178.6 (s); (O₂CP(*t*-Bu)₂) 189.1 ppm (d, ¹J_{31P-13C} = 27 Hz). ³¹P{¹H} NMR (room temperature, toluene-*d*₈): δ 44.4 ppm (s).

W₂(O₂CNMe₂)₂(O₂CPCy₂)₂(NMe₂)₂ (IIc). IIc was prepared as described for the solid-state preparation of IIb from 1,2-W₂(NMe₂)₄(PCy₂)₂ (350 mg, 0.373 mmol) and 1.50 mmol of CO₂. Only 55 mg (13%) of IIc (80% pure by NMR) were isolated by recrystallization in hexane at -20 °C due to subsequent isomerization to V. NMR tube scale reactions (30 mg of 1,2-W₂(NMe₂)₄(PCy₂)₂ in 0.5 mL of toluene-*d*₈) demonstrate the clean formation of IIc, but this is seen to isomerize the VI overnight at room temperature or to V after several days at -20 °C. ¹H NMR (room temperature, toluene-*d*₈): δ (O₂CN(CH₃)₂) 2.48 (d, ³J_{13C-1H} = 2.2 Hz) and 2.72 (d, ³J_{13C-1H} = 2.2 Hz); δ (N(CH₃)₂) 3.10 (s) and 4.91 ppm (s). ¹³C NMR (room temperature, toluene-*d*₈): δ (O₂CNMe₂) 179.0 (s); δ (O₂CPCy₂) 189.9 (d, ¹J_{31P-13C} = 20 Hz). ³¹P NMR (room temperature, toluene-*d*₈): δ 9.1 ppm (s).

Synthesis of V. 1,2-W₂(NMe₂)₄(PCy₂)₂ (300 mg, 0.320 mmol) was taken up in toluene (3 mL), and CO₂ (>4 equiv) was condensed onto the frozen reaction mixture. The solution was thawed at -78 °C with stirring for 2 1/2 h. A small amount of precipitate was filtered from the reddish brown solution, the extract was allowed to slowly warm to -20 °C, and within 24 h a fine orange precipitate began to form. The total isolated yield was 65 mg (18%). By monitoring this reaction (¹H NMR) the initial formation of IIc is observed followed by the gradual isomerization or decomposition to V and other minor products over a period of several days at -20 °C. V is insoluble in hexane and moderately soluble in toluene. IR for V (KBr, cm⁻¹): 2923 (s), 2855 (s), 2780 (w), 1672 (s), 1591 (s), 1575 (s), 1489 (m), 1448 (m), 1397 (s), 1267 (m), 1234 (s), 1181 (m), 1165 (m), 1127 (w), 1036 (w), 1001 (w), 941 (m), 888 (w), 849 (w), 817 (m), 791 (m), 738 (w), 660 (m). IR for ¹³CO₂-labeled V (KBr pellet, cm⁻¹): 2928 (s), 2853 (s), 2773 (w), 1634 (s), 1564 (s), 1553 (s), 1452 (m), 1410 (m), 1388 (s), 1257 (m), 1221 (s), 1179 (w), 1143 (m), 1126 (m), 1032 (w), 1001 (w), 941 (m), 889 (w), 849 (w), 806 (w), 766 (w), 672 (m). ¹H NMR (room temperature, toluene-*d*₈): δ (NCH₃)₂ 2.76 (d, ³J_{31P-1H} = 2.2 Hz) and 4.28 (d, ³J_{31P-1H} = 2.8 Hz); (O₂CN(CH₃)₂) 2.5 (br) and 3.1 ppm (br). ¹H NMR (-40 °C, toluene-*d*₈): δ (N(CH₃)₂) 2.69 (d, ³J_{31P-1H} = 1.0 Hz) and 4.29 (d, ³J_{31P-1H} = 2.0 Hz); (O₂CN(CH₃)₂) 2.56 (³J_{13C-1H} = 3.0 Hz) and 3.06 ppm (d, ³J_{13C-1H} = 2.6 Hz). ¹³C{¹H} NMR (room temperature, toluene-*d*₈): δ (O₂CNMe₂) 161.5 (s); (O₂C(PCy₂)₂) 182.7 ppm (d, ¹J_{31P-13C} = 58.9 Hz). ³¹P{¹H} NMR: δ 72.1 ppm (s, ¹J_{183W-31P} = 230 Hz, 14%).

Synthesis of VI. W₂(NMe₂)₄(PCy₂)₂ (150 mg, 0.160 mmol) was taken up in toluene (2 mL) and 4 equiv (0.640 mmol) of CO₂ was condensed onto the frozen reaction mixture. The solution was warmed to room temperature, and after 24 h 68 mg (38%) of a dark orange microcrystalline material VI was isolated. This product is insoluble in hexane and only very sparingly soluble in toluene and benzene. ¹H NMR in benzene-*d*₆ of crystals washed with hexane show the presence of toluene solvate molecules, consistent with the elemental analysis. Anal. Calcd for W₂C₃₆H₆₈N₄O₈P₂·1/2C₇H₈ (1160.8): C, 40.87; H, 6.26; N, 4.83. Found: C, 41.20; H, 6.17; N, 4.53. IR for VI (KBr, cm⁻¹): 2922 (s), 2858 (m), 2833 (w), 2778 (w), 1672 (s), 1589 (s), 1574 (s), 1492 (m), 1447 (m), 1396 (s), 1268 (m), 1235 (s), 1208 (m), 1172 (s), 1123 (w), 1033 (w), 1001 (w), 941 (m), 885 (w), 850 (w), 822 (m), 790 (w), 744 (w), 658 (m). IR for ¹³CO₂-labeled VI (KBr, cm⁻¹): 2922 (s), 2848 (m), 2821 (w), 2778 (w), 1630 (s), 1554 (s), 1444 (m), 1387 (s), 1266 (m), 1224 (s), 1151 (m), 1122 (w), 1032 (w), 1001 (w), 941 (m), 888 (w), 850 (w), 807 (m), 762 (w), 657 (m). ¹H NMR for VI (room temperature, toluene-*d*₈): δ (NCH₃)₂ 3.07 (⁴J_{31P-1H} = 2.0 Hz) and 4.62 ppm (³J_{31P-1H} = 2.3 Hz). ¹H NMR (45 °C, toluene-*d*₈): δ (N(CH₃)₂) 3.06 (d, ³J_{31P-1H} = 2.3 Hz) and 4.62 (d, ⁴J_{31P-1H} = 2.0 Hz); (O₂CN(CH₃)₂) 2.66 ppm (s, br). ¹³C NMR for VI (room temperature, toluene-*d*₈): δ (O₂CNMe₂) 161.4 (s); (O₂CPCy₂) 181.2 ppm (d, ¹J_{31P-13C} = 56.3 Hz). ³¹P NMR for VI (room temperature, toluene-*d*₈): δ 76.1 ppm (s, ¹J_{183W-31P} = 247 Hz, 14%).

1,2-W₂(NMe₂)₄(P(*t*-Bu)₂)₂ + 1 ¹³CO₂. W₂(NMe₂)₄(P(*t*-Bu)₂)₂ (30 mg, 0.036 mmol) was placed into an NMR tube and dissolved in 0.5 mL of a 50:50 mixture of toluene-*d*₈/Freon-12. After 1 equiv (0.036 mmol) of ¹³CO₂ was condensed into the NMR tube, it was flame sealed and the reaction mixture was allowed to thaw at -120 °C in an EtOH/liquid N₂ slush bath. After 1/2 h at -120 °C the NMR tube was placed into a broad-band NMR probe, precooled to -120 °C, allowing the measurement of both the ¹³C and ³¹P spectra. ¹³C{¹H} (-120 °C, toluene-*d*₈/Freon-12): major resonance δ 197.3 ppm (d, ¹J_{31P-13C} = 39.3 Hz); minor resonances δ 194.0 (d, ¹J_{31P-13C} = 36.3 Hz); 186.7 (br d, ¹J_{31P-13C} = 54.8

(20) Jones, R. A.; Fasch, J. G.; Norman, N. C.; Wittlesey, B. R.; Wright, T. C. *J. Am. Chem. Soc.* 1983, 105, 6184.

Hz); 183.5 (d, $^1J_{31\text{P}-^{13}\text{C}} = 25.2$ Hz); 181.8 ppm (d, $^1J_{31\text{P}-^{13}\text{C}} = 33.8$ Hz). $^{31}\text{P}\{^1\text{H}\}$ NMR using 1 equiv of $^{13}\text{CO}_2$ (-120 °C, toluene-*d*₆/Freon-12) major product δ 38.2 ppm (s, $^1J_{183\text{W}-^{31}\text{P}} = 116$ Hz, 14%); minor products δ 85.1 (s); 84.5 (s); 42.7* (s); 41.1 (s); 40.1 (br s); 39.4 (br s); 34.3 ppm* (s). Chemical shifts denoted with an * do not exhibit coupling to ^{13}C when $^{13}\text{CO}_2$ is used.

$\text{W}_2(\text{NMe}_2)_2(\text{P}(t\text{-Bu})_2)_2 + 4\ ^{13}\text{CO}_2 + \text{HPCy}_2$. An NMR tube was charged with $\text{W}_2(\text{NMe}_2)_2(\text{P}(t\text{-Bu})_2)_2$ (20 mg, 0.024 mmol) and HPCy_2 (5 μL , ≥ 1 equiv) in a solution of 0.5 mL of toluene-*d*₆. After $^{13}\text{CO}_2$ (4 equiv) was condensed into the NMR tube, it was flame sealed and warmed to room temperature. ^{31}P NMR and ^{13}C NMR exhibit only the chemical shifts of IIb, free HPCy_2 , and a trace of free $\text{HP}(t\text{-Bu})_2$. No significant change in the reaction mixture was observed over 1 week at ambient temperature.

$\text{W}_2(\text{O}_2\text{CNMe}_2)_2(\text{O}_2\text{CP}(t\text{-Bu})_2)_2(\text{NMe}_2)_2 + ^{13}\text{CO}_2$. An NMR tube was charged with a solution of 30 mg (0.030 mmol) of IIb in 0.5 mL of toluene-*d*₆. After $^{13}\text{CO}_2$ (6 equiv, 0.178 mmol) was condensed into the NMR tube, it was flame sealed and warmed to room temperature. This reaction has never been observed to go to completion (30–50% by NMR), leaving in solution a mixture of IIb and the new product IV. ^1H NMR of IV (room temperature, toluene-*d*₆): δ ($\text{O}_2\text{CP}(t\text{-Bu})_2$) 1.49 (d, $^3J_{31\text{P}-^1\text{H}} = 11.6$ Hz); ($\text{O}_2\text{CN}(\text{CH}_3)_2$) 2.4 (apparent t (s with $^{12}\text{CO}_2$), $^3J_{13\text{C}-^1\text{H}} = 2.9$ Hz) and 2.83 ppm (apparent t (s with $^{12}\text{CO}_2$), $^3J_{13\text{C}-^1\text{H}} = 2.5$ Hz). Note chemical shifts corresponding to the IIb remaining in solution have been subtracted from the total spectrum to identify the chemical shifts of IV. ^{13}C NMR of IV (room temperature, toluene-*d*₆): δ (O_2CNMe_2) 164.9 (s) and 181.0 (s); ($\text{O}_2\text{CP}(t\text{-Bu})_2$) 190.3 ppm (d, $^1J_{31\text{P}-^{13}\text{C}} = 27.6$ Hz). There is no evidence for $^{13}\text{CO}_2$ incorporation into the IIb remaining in solution. $^{31}\text{P}\{^1\text{H}\}$ NMR (room temperature, toluene-*d*₆): δ (IIb) 44.4 (s); 43.7 (s, br) and 42.7 ppm (s, br).

$\text{W}_2(\text{O}_2\text{CNMe}_2)_2(\text{O}_2\text{CP}(t\text{-Bu})_2)_2(\text{NMe}_2)_2 + 6\ ^{13}\text{CO}_2 + \text{HPCy}_2$. IIb (24 mg, 0.024 mmol) and HPCy_2 (5 μL , > 1 equiv) were taken up in 0.5 mL of toluene-*d*₆ in an NMR tube. After $^{13}\text{CO}_2$ (6 equiv, 0.143 mmol) was condensed into the NMR tube, it was flame sealed and warmed to room temperature. No PCy_2 for $\text{P}(t\text{-Bu})_2$ exchange was observed. The resulting reaction mixture was the same as that described above for the reaction IIb with $^{13}\text{CO}_2$ except for the presence of free HPCy_2 .

$\text{Mo}_2(\text{O}_2\text{CNMe}_2)_2(\text{O}_2\text{CP}(t\text{-Bu})_2)_2(\text{NMe}_2)_2 + 6\ ^{13}\text{CO}_2$. IIa (20 mg, 0.024 mmol), in a solution of 0.5 mL of toluene-*d*₆, was added to an NMR tube. After $^{13}\text{CO}_2$ (6 equiv, 0.144 mmol) was condensed into the NMR tube, it was flame sealed and warmed to room temperature. No reaction was observed until the onset of decomposition after 24 h at ambient temperature. The room temperature $^{31}\text{P}\{^1\text{H}\}$ spectrum shows several decomposition products with chemical shifts ranging from 44 and 59 ppm, several of which show $^{31}\text{P}-^{13}\text{C}$ coupling of approximately 30 Hz. The $^{13}\text{C}\{^1\text{H}\}$ spectrum likewise confirms the incorporation of $^{13}\text{CO}_2$ into phosphinecarboxylates (doublets between 185 and 195 ppm) and demonstrates the incorporation into carbamates ligands (singlets between 165 and 175 ppm).

$\text{Mo}_2(\text{O}_2\text{CNMe}_2)_2(\text{O}_2\text{CP}(t\text{-Bu})_2)_2(\text{NMe}_2)_2 + 6\ ^{13}\text{CO}_2 + \text{HPCy}_2$. An NMR tube was charged with IIa (15 mg, 0.017 mmol) and HPCy_2 (5 μL , > 1 equiv) which was dissolved in 0.5 mL of toluene-*d*₆. After $^{13}\text{CO}_2$ (6 equiv, 0.102 mmol) was condensed into the NMR tube, it was flame sealed and warmed to room temperature. No reaction was observed except the onset of decomposition after 24 h at ambient temperature. $^{31}\text{P}\{^1\text{H}\}$ NMR and $^{13}\text{C}\{^1\text{H}\}$ NMR are similar to that previously described for the reaction of IIa with $^{13}\text{CO}_2$ save the appearance of two dicyclohexyl phosphinecarboxylate doublets in the ^{31}P NMR spectrum at 7.7 and 18.9 ppm and the presence of an excess of free HPCy_2 .

$\text{Mo}_2[\text{O}_2\text{CP}(t\text{-Bu})_2]_4 + 6\ ^{13}\text{CO}_2$. An NMR tube was charged with III (15 mg, 0.014 mmol) in a solution of 0.5 mL of toluene-*d*₆. After $^{13}\text{CO}_2$ (6 equiv, 0.084 mmol) was condensed into the NMR tube, it was flame sealed and warmed to room temperature. No reaction was observed over the course of several weeks at ambient conditions.

$\text{Mo}_2[\text{O}_2\text{CP}(t\text{-Bu})_2]_4 + 6\ ^{13}\text{CO}_2 + \text{HPCy}_2$. An NMR tube was charged with III (15 mg, 0.014 mmol) and HPCy_2 (2.5 μL , 1 equiv) in 0.5 mL of toluene-*d*₆. After $^{13}\text{CO}_2$ (6 equiv, 0.084 mmol) was condensed into the NMR tube, it was flame sealed and warmed to room temperature. No reaction was observed over the course of several weeks.

Crystallographic Studies. General operating procedures and a listing of programs have been published.²¹ A summary of crystal data is given in Table VII.

$\text{Mo}_2(\text{O}_2\text{CP}(t\text{-Bu})_2)_4 \cdot 2\text{C}_6\text{H}_6$. A suitable crystal was located and transferred to the goniostat by standard inert atmosphere handling techniques employed by the IUMSC and cooled to -155 °C for characterization and data collection. The sample was reported to be air-stable for prolonged periods of time, and examination of the remaining sample

Table VII. Summary of Crystal Data

	III	IIb
empirical formula	$\text{Mo}_2\text{C}_{48}\text{H}_{84}\text{O}_8\text{P}_4$	$\text{C}_{28}\text{H}_{60}\text{N}_4\text{O}_8\text{P}_2\text{W}_2$
crystal color	colorless	light tan
crystal dimens, mm	$0.25 \times 0.25 \times 0.30$	$0.20 \times 0.18 \times 0.08$
space group	$P2_1/n$	$P\bar{1}$
cell dimens		
temp, °C	-155	-151
a, Å	13.731 (21)	15.455 (7)
b, Å	12.789 (17)	15.786 (7)
c, Å	15.835 (23)	8.502 (4)
α , deg		97.22 (2)
β , deg	94.86 (8)	97.86 (2)
γ , deg		101.22 (2)
Z, molecules/cell	2	2
vol, Å ³	2770.76	1990.63
D_{calcd} , gm/cm ³	1.324	1.686
λ , Å	0.710 69	0.710 69
MW	1104.96	1104.45
linear abs coeff, cm ⁻¹	5.993	60.215
detector to sample dist, cm	22.5	22.5
sample to source dist, cm	23.5	23.5
av θ scan width at halfheight	0.25	0.25
scan speed, deg/min	4.0	6.0
scan width deg + dispersn	2.0	1.8
individ bkgd, s	6	6
aperture size, mm	3.0×4.0	3.0×4.0
2θ range, deg	6–45	6–45
total no. of relcns collected	4401	5941
no. of unique intensities	3633	5173
no. with $F > 0.0$		4640
no. with $F > 3.00\sigma(F)$	2943	4153
$R(F)$	0.0324	0.0746
$R_w(F)$	0.0350	0.0707
goodness of fit for the last cycle	0.870	1.666
max δ/σ for last cycle	0.05	0.169

after the crystal was mounted confirmed this.

A systematic search of a limited hemisphere of reciprocal space located a set of diffraction maxima with symmetry and systematic absences corresponding to the unique monoclinic space group $P2_1/n$. Subsequent solution and refinement of the structure confirmed this choice. Data were collected in the usual manner by using a continuous θ - 2θ scan with fixed backgrounds. Data were reduced to a unique set of intensities and associated σ 's in the usual manner.

The structure was solved by a combination of direct methods (MULTAN78) and Fourier techniques. The positions of all hydrogen atoms were clearly visible in a difference Fourier phased on the non-hydrogen atoms, and the coordinates and isotropic thermal parameters for hydrogens were varied in the final cycles of refinement. No absorption correction was performed. A final difference Fourier was essentially featureless, with the largest peak being $0.53 \text{ e}/\text{\AA}^3$.

$\text{W}_2(\text{O}_2\text{CNMe}_2)_2(\text{O}_2\text{CP}(t\text{-Bu})_2)_2(\text{NMe}_2)_2$. The sample consisted of relatively large tannish-yellow crystals coated with black, oily-looking, sticky material. The crystals were all quite flat, and a small fragment was cleaved from a larger crystal. The crystal still was coated with some of the black stuff, but was transferred to the goniostat where it was cooled to -151 °C for characterization and data collection. A systematic search of a limited hemisphere of reciprocal space yielded a set of reflections that showed no symmetry (other than a center of inversion) and no systematic extinctions. The reflections were indexed on a triclinic lattice and the choice of the centrosymmetric space group $P\bar{1}$ was confirmed by the solution and refinement of the structure. Data collection was carried out as described in Table IV. After data reduction and averaging of equivalent reflections, a unique set of 5173 reflections remained, and of these, 4153 were considered observed by the criterion $F \geq 3.0\sigma(F)$. The R for the averaging was 0.033 for 688 reflections measured more than once.

The structure was solved by locating the two W atoms by means of MULTAN; the remaining non-hydrogen atoms of the structure were located in difference Fourier phased with the already located atoms. It was not possible to locate hydrogen atoms as the difference maps persistently had peaks of approximately $2 \text{ e}/\text{\AA}^3$ within 1 Å of the W atoms. Hydrogen atoms were introduced in fixed calculated positions and the full-matrix least-squares refinement was completed by using anisotropic thermal parameters on the non-hydrogen atoms. There appears to be some abnormalities in the bond distances in the two phosphinecarboxylate groups.

(21) Chisholm, M. H.; Foltling, K.; Huffman, J. C.; Kirkpatrick, C. C. *Inorg. Chem.* 1984, 23, 1023.

These might possibly be due to an incomplete absorption correction; however, attempts at improving the correction did not improve the bonds. Looking at the ORTEP plots it is evident that the groups at P(36) definitely have much larger thermal vibrations. The weakly bonded W-O distances are W(1)-O(20) = 2.635 (17) Å and W(2)-O(35) = 2.708 (14) Å. The closest intramolecular contact for the two non-bonded O's are O(20)-O(3) = 2.92 Å and O(35)-O(11) = 2.99 Å. The closest intermolecular contacts are O(20) to C(24) = 4.21 Å and O(35) to C(8) = 3.29 Å.

The final difference map still had several peaks of $\sim 2.5 \text{ e}/\text{\AA}^3$ in the close vicinity of the W atoms. The molecule has an approximate 2-fold axis perpendicular to the W(1)-W(2) bond.

Acknowledgment. We thank the National Science Foundation for support. W.E.B. acknowledges a Chester Davis Fellowship for 1986-1987.

Supplementary Material Available: Tables of anisotropic thermal parameters, bond distances, and bond angles for $\text{Mo}_2(\text{O}_2\text{CP}(t\text{-Bu})_2)_4 \cdot 2\text{C}_6\text{H}_6$ and $\text{W}_2(\text{NMe}_2)_2(\text{O}_2\text{CNMe}_2)_2(\text{O}_2\text{CP}(t\text{-Bu})_2)_2$ (11 pages); observed and calculated structure factors (19 pages). Ordering information is given on any current masthead page.

Ligand Dependence of Electronic Configuration of the Rh-Rh Bond in Rh_2^{5+} Complexes As Studied by Electron Spin Resonance and Electrochemistry

Takashi Kawamura,^{*1a} Hiroaki Katayama,^{1b} Hiroyuki Nishikawa,^{1c} and Tokio Yamabe^{1b,c}

Contribution from the Department of Chemistry, Faculty of Engineering, Gifu University, Yanagido, Gifu 501-11, Japan, and the Division of Molecular Engineering and the Department of Hydrocarbon Chemistry, Faculty of Engineering, Kyoto University, Kyoto 606, Japan.
Received February 20, 1989

Abstract: Electron spin resonance spectra of Rh_2^{5+} radicals derived from $\text{Rh}_2(\text{O}_2\text{CCH}_3)_4\text{L}_2$, where L is H_2O , CH_3OH , *i*-PrOH, THF, $(\text{CH}_3)_2\text{CO}$, CH_3CN , and Cl^- , show abnormally large shifts of the principal values of their g tensors from the free-spin value ($g_e = 2.0023$): $g_{\parallel} = 3.38\text{--}4.00$ and $g_{\perp} = 0.6\text{--}1.87$. These large shifts indicate that the orbital angular momentum of the odd electron in these radicals is not quenched; namely the odd-electron orbital is degenerate. The assignment of $\sigma^2\pi^4\delta^2\pi^*2\pi^*3$ to the electronic configuration of their Rh-Rh bonds is the most reasonable one satisfying these observations. Cationic radicals generated from $\text{Rh}_2(\text{O}_2\text{CCH}_3)_{4-n}[\text{CH}_3\text{C}(\text{O})\text{NH}]_n(\text{CH}_3\text{CN})_2$, where $n = 1\text{--}4$, have been reported to have $g_{\parallel} < g_e$ and $g_{\perp} > g_e$. This is consistent with the electronic configuration of $\sigma^2\pi^4\delta^2\pi^*4\delta^*1$ for their Rh-Rh bonds. Those Rh_2^{4+} complexes, of which Rh_2^{5+} radicals have an odd electron accommodated in the π_{RhRh}^* orbital, have high oxidation potentials (0.58-0.77 V vs Fc^+/Fc , where Fc designates ferrocene). Those Rh_2^{4+} complexes, of which Rh_2^{5+} radicals have an odd electron in the δ_{RhRh}^* orbital, show low oxidation potentials (-0.33 to +0.49 V vs Fc^+/Fc). The latter complexes have amidate or amidinate bridging ligands. These observations show that a substitution of amidate or amidinate ligands for bridging carboxylates results in an enhanced destabilization of the δ_{RhRh}^* orbital. This destabilization should be induced by an increased mixing of ligand π orbitals into the δ_{RhRh}^* orbital in a π -antibonding phase between the Rh atom and the bridging ligand. An appreciable delocalization of the σ_{RhRh} orbital onto bridging ligands is also proposed in connection with a dependence of oxidation potentials on bridging ligands.

Over the past two decades a substantial number of reports have appeared describing preparations and accurate geometries of Rh_2^{4+} complexes.²⁻⁷ Spectroscopic characterizations of this class of complexes lend insight into electronic structures of metal-metal bonds. Electron spin resonance (ESR) studies of Rh_2^{5+} complexes have shown an unexpected dependence of the electronic configuration of the Rh-Rh bond on the ligands. Complexes with axial ligands of phosphines and phosphites^{8,9} have been shown to have

the electronic configuration of $\pi^4\delta^2\delta^*2\pi^*4\sigma^1$.⁸ This has been reproduced by molecular orbital calculations.^{10,11}

The configuration of the Rh-Rh bond in $[\text{Rh}_2(\text{O}_2\text{CCH}_3)_4(\text{H}_2\text{O})_2]^{4+}$ has been calculated to be $\sigma^2\pi^4\delta^2\pi^*4\delta^*1$ by an SCF-X α -SW method¹² and to be $\pi^4\delta^2\delta^*2\pi^*4\sigma^1$ by an ab initio unrestricted Hartree-Fock method,¹¹ respectively. In contrast to both of the predictions, our preliminary ESR study has shown that this aquo complex has the configuration of $\sigma^2\pi^4\delta^2\pi^*2\pi^*3$.¹³ Subsequently this experimental result has been reproduced by calculations with an ab initio Hartree-Fock CI method.¹⁴ The CI expansion has been necessary to describe *localization* of positive

(1) (a) Gifu University. (b) The Division of Molecular Engineering, Kyoto University. (c) The Department of Hydrocarbon Chemistry, Kyoto University.

(2) Cotton, F. A.; Walton, R. A. *Multiple Bonds Between Metal Atoms*; Wiley-Interscience: New York, 1982.

(3) Felthouse, T. R. *Prog. Inorg. Chem.* **1982**, *29*, 73.

(4) Boyer, E. B.; Robinson, S. D. *Coord. Chem. Rev.* **1983**, *50*, 109.

(5) Lifsey, R. S.; Lin, X. Q.; Chavan, M. Y.; Ahsan, M. Q.; Kadish, K. M.; Bear, J. L. *Inorg. Chem.* **1987**, *26*, 830, and references cited therein.

(6) Piraino, P.; Bruno, G.; Tresoldi, G.; Lo Schiavo, S.; Zanello, P. *Inorg. Chem.* **1987**, *26*, 91.

(7) Dunbar, K. R. *J. Am. Chem. Soc.* **1988**, *110*, 8247.

(8) (a) Kawamura, T.; Fukamachi, K.; Hayashida, S. *J. Chem. Soc., Chem. Commun.* **1979**, 945. (b) Kawamura, T.; Fukamachi, K.; Sowa, T.; Hayashida, S.; Yonezawa, T. *J. Am. Chem. Soc.* **1981**, *103*, 364.

(9) Chavan, M. Y.; Zhu, T. P.; Lin, X. Q.; Ahsan, M. Q.; Bear, J. L.; Kadish, K. M. *Inorg. Chem.* **1984**, *23*, 4538.

(10) Burnsten, B. E.; Cotton, F. A. *Inorg. Chem.* **1981**, *20*, 3042.

(11) Nakatsujii, H.; Onishi, Y.; Ushio, J.; Yonezawa, T. *Inorg. Chem.* **1983**, *22*, 1623.

(12) Norman, J. D., Jr.; Renzoni, G. E.; Case, D. A. *J. Am. Chem. Soc.* **1979**, *101*, 5256.

(13) Kawamura, T.; Katayama, H.; Yamabe, T. *Chem. Phys. Lett.* **1986**, *130*, 20.

(14) Mougnot, P.; Demuyneck, J.; Bénard, M. *Chem. Phys. Lett.* **1987**, *136*, 279.